IJE TRANSACTIONS A: Basics Vol. 33, No. 7, (July 2020) 1364-1374

International Journal of Engineering

Journal Homepage: www.ije.ir

Meshing Error of Elliptic Cylinder Gear Based on Tooth Contact Analysis

D. Changbin*, L. Yongping, W. Yongqiao

School of Mechanical and Electronical Engineering, Lanzhou University of Technology, Lanzhou, China

PAPER INFO

Paper history:
Received 21 February 2020
Received in revised form 09 March 2020
Accepted 12 July 2020

Keywords:
Elliptical Cylinder Gear
Static Contact
Finite Element Analysis
Dynamic Meshing Characteristics
Meshing Error

ABSTRACT

In order to study the dynamic meshing characteristics of the elliptic cylinder gear and obtain the meshing error of the gear transmission system, the two-dimensional static contact analysis of the gear tooth surface is carried out using ANSYS software, and the key parts of the contact area of the tooth surface are determined. Then, the dynamic meshing model of the elliptic cylinder gear is established and the dynamic contact process under load is simulated by ANSYS LS-DYNA software. The distribution law of effective plastic strain, effective stress and pressure of the driving and driven wheels are obtained. On this basis, the distribution law of meshing error is obtained by calculation. The results show that the distribution of stress, strain and tooth surface pressure during tooth meshing is related to the position of the tooth on the elliptical pitch curve. The position of the tooth on the pitch curve and the load it bears has a certain influence on the meshing error. The results of this research can provide some guidance for subsequent study of transmission error of non-circular gears, gears modification and engineering applications.

doi: *10.5829/ije.2020.33.07a.24*

1. INTRODUCTION

Non-circular cylinder gears are distinguished from cylinder gears by their non-circular pitch curves. As one of the simplest non-circular cylinder gears, the elliptic cylinder gears are compact and widely used in robots, printers, fans and hydraulic motors [1]. In view of its wide range of applications, it is of practical value to study the meshing characteristics and meshing errors of elliptic cylinder gears. At present, static contact or incomplete gear model are mostly used to analyze the meshing characteristics of gears, while the tooth profiles of elliptic cylinder gears are different. In view of the above situation, this paper analyzes and establishes the dynamic meshing model of the elliptic cylinder gear to simulate the actual working condition of the gear under the load. Compared with static contact analysis, dynamic contact analysis is more accurate.

The small tooth profile error, manufacturing error, installation error and center-to-center error will cause the involute gear to generate a lot of vibration and noise during the meshing process [2], and those errors are transmitted and accumulated by teeth meshing. Therefore, it is necessary to study the meshing errors existing in the gear meshing process. As a kind of gear transmission error, the meshing error has received extensive attention in recent years, and a lot of research results have been accumulated for the gear transmission error. Among them, Sainte et al. [3], aimed at spur gear and helical gear, studied the relationship between the dynamic transmission error and the load it bears. Sungho et al.[4] obtained the dynamic transmission error of the gear by simulating the loaded tooth contact, and proposed the dynamic transmission error of the gear as a basis for fault diagnosis. Hotait et al. [5] studied the relationship between dynamic transmission error and dynamic stress coefficient in spur gear pairs. Wang et al. [6] studied the dynamic transmission error of eccentric cylinder gears under consideration of time-varying backlash caused by gear eccentricity and load variation. Yu et al. [7] proposed a double eccentric gear model for calculating the transmission error caused by the gear eccentricity error and the transmission error caused by

*Corresponding Author's Email: *lutdcb@126.com* (D. Changbin)

Please cite this article as: D. Changbin, L. Yongping, W. Yongqiao, Meshing Error of Elliptic Cylinder Gear Based on Tooth Contact Analysis, International Journal of Engineering (IJE), IJE TRANSACTIONS A: Basics Vol. 33, No. 7, (July 2020) 1364-1374

the eccentricity error can be predicted by obtaining the transmission error of the designed gap compensation device. Deng et al.[8] proposed a model for synchronously measuring the gear transmission curve in the time-scale domain, and solved the jump error of the transmission error curve in the time domain and applied it to the measurement of the hypoid gear transmission error. Zou et al. [9] established an analytical calculation model for transmission error of the involute gear pairs with double eccentricity error, and studied the dynamic transmission error of the eccentric gear. Wu et al. [10] studied the effects of installation error, eccentricity error and meshing error on the uniform load characteristics of the system by establishing a nonlinear dynamic model of the planetary gear train. Chang et al. [11] studied the gear meshing error and pointed out that the deformation during the gear meshing can be divided into two parts: linear macroscopic deformation and nonlinear local deformation, and studied the influence of different error types and distribution forms on system vibration.

Most practical problems are difficult to get accurate solutions for. While the finite element method not only has high calculation accuracy, but also can adapt to a variety of complex shapes.Therefore, it has become an effective engineering analysis method. As far as the current dynamic analysis methods are concerned, most of them adopt the finite element simulation method [12-14]. The most widely used analysis software in the gear meshing analysis process is LS-DYNA, which is probably the most famous universal explicit dynamic analysis program in the world. It can simulate various complex problems in the real world, and is especially suitable for solving nonlinear dynamic shock problems such as high-speed collisions, explosions, and metal forming of various 2D and 3D nonlinear structures. At the same time, it can solve heat transfer, fluid, and fluid-solid coupling problems [15-17].

The above literatures are all concerned with the transmission error of gears, and there are few reports on the study of meshing errors between teeth. Generally, the gear transmission error is analyzed for the displacement or rotation angle between the input and output shafts, and the deformation between the shaft and the gear is not considered. Considering the meshing error of the gear pair, the problem of load deformation and meshing of the gear under the meshing error state is analyzed, which makes the gear meshing more in line with the actual situation. Therefore, the paper proposes that the difference of strain, stress and pressure at the same meshing unit between the driving and driven wheels is used as the meshing error. Taking a pair of elliptic cylinder gear as the research object, the meshing error of the elliptic cylinder gear is studied by simulating the actual meshing process of the gear.

This work is organized as follows. Section 2 introduces the mathematical model and finite element analysis theory of elliptic cylinder gear tooth surface. Section 3 introduces the static contact analysis of tooth surface. Section 4 proposes the dynamic meshing model of elliptic cylinder gear and introduces the dynamic contact analysis of gears and the distribution law of meshing error. Finally, Section 5 provides the conclusions. Figure 1 shows the flow chart of the research process.

2 ELLIPTIC CYLINDER GEAR TOOTH SURFACE MODEL AND FINITE ELEMENT ANALYSIS THEORY

2. 1. Elliptic Cylinder Gear Tooth Surface Model

The tooth surface of the elliptic cylinder gear is an involute surface, the end face of the tooth is an involute, and the tooth profile of the elliptic cylinder gear can be determined by the involute of the tooth profile. The vector equation of the tooth profile is [1]:

$$\boldsymbol{r}_f = \boldsymbol{r}_g + \boldsymbol{an} \tag{1}$$

where $\boldsymbol{r}_f$ is the radial diameter of any point n on the tooth profile. $\boldsymbol{r}_g$ is the radial diameter of the pitch curve at the intersection of the normal and pitch curve on point n of the tooth profile. $\boldsymbol{an}$ indicates that the direction is consistent with the normal direction of the tooth profile, and the length is equal to the section curve and the tooth profile vector of distance. The tooth profile of the elliptic cylinder gear can be divided into two points, which are higher than the pitch curve and

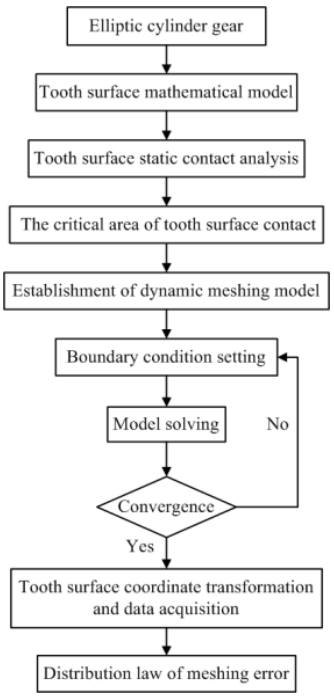

Figure 1. The flow chart of the research process

lower than the pitch curve. For the two-part tooth profile equation, there are different methods [1]. Figures 2 and 3 are the equations of the tooth profile above the pitch curve and below the pitch curve respectively, where the right tooth profile angle is $\theta-\mu\pm\alpha_u$, and the left tooth profile angle is $\mu-\theta\pm\alpha_u$ (+,- representing above the pitch curve point and below the pitch curve point, respectively).

The equation of the left and right tooth profiles is extended to the three-dimensional space to obtain the tooth surface equation of the elliptic cylinder gear, wherein the right tooth surface equation is:

$$\begin{cases} x_R = r_g\cos\theta \pm an\cos(\theta-\mu+\alpha_\mu) \\ y_R = r_g\sin\theta \pm an\sin(\theta-\mu+\alpha_\mu) \\ z_R = z_i \end{cases} \quad (2)$$

And the left tooth surface equation of the elliptic cylinder gear is:

$$\begin{cases} x_L = r_g\cos\theta \mp a'n'\cos(\mu-\theta-\alpha_u) \\ y_L = r_g\sin\theta \mp a'n'\sin(\mu-\theta-\alpha_u) \\ z_L = z_i \end{cases} \quad (3)$$

where, (x_R, y_R, z_R) represents the right gear surface coordinate, (x_L, y_L, z_L) represents the left gear surface coordinate, z_i refers to the direction of the tooth line and is equal to the width of the tooth, α_μ the profile pressure angle, μ the angle between the pitch curve diameter and the pitch curve tangent of point *a* [18].

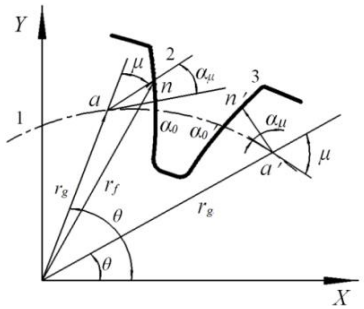

Figure 2. Tooth profile above the pitch curve

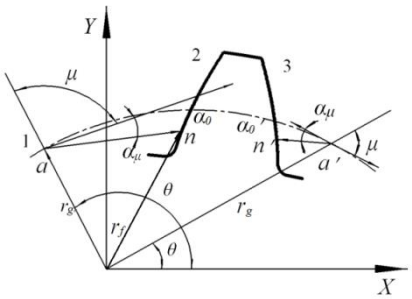

Figure 3. Tooth profile below the pitch curve

2. 2. Finite Element Analysis Theory The basic motion equation of the gear system dynamics analysis is:

$$M\ddot{U}+C\dot{U}+KU=F \quad (4)$$

where M, C, K and F are the mass matrix, damping matrix, stiffness matrix. U, $\dot{U}$ and $\ddot{U}$ are the displacement vector, velocity, and acceleration of the nodes, respectively.

As one of the post-processing softwares of ANSYS LS-DYNA, LS-PREPOST uses the central difference method to solve the motion differential equation of dynamic problems. The essence of the central difference method is to replace the differential with the difference, namely:

$$\begin{cases} \ddot{U}_t = \dfrac{1}{\Delta t^2}(U_{t-\Delta t}-2U_t+U_{t+\Delta t}) \\ \dot{U}_t = \dfrac{1}{2\Delta T}(-U_{t-\Delta t}+U_{t+\Delta t}) \end{cases} \quad (5)$$

Taking Equation (5) into dynamic differential Equation (4), the system of linear equations can be obtained

$$\bar{M}U_{t+\Delta t}=\bar{R}_t \quad (6)$$

$$\bar{M}=\frac{1}{\Delta t_2}M+\frac{1}{2\Delta t}C \quad (7)$$

$$\bar{R}_t=F_t-(K-\frac{2}{\Delta t^2}M)U_t-(\frac{1}{\Delta t^2}M-\frac{1}{2\Delta t}C)U_{t-\Delta t} \quad (8)$$

where $\bar{M}$ is the effective mass matrix and $\bar{R}_t$ is the effective load vector.

According to Equation (6), the state parameters of $t+\Delta t$ time can be calculated from the state quantities of $t-\Delta t$ and t time, which is the characteristic of display algorithm.

The time step of the display calculation is limited by the element size, and a reasonable and accurate finite element model needs to be established to improve the calculation accuracy [18]. In contrast, LS-PREPOST software is used to simulate the dynamic meshing process of the gear by establishing a non-linear contact unit in the meshing area. On this basis, gear deformation, transmission error, and gear stress can be obtained at the same time, which avoided the complicated writing and calculation of finite element programs, and can be applied here for research on the meshing error of elliptic cylindrical gear. Figure 4 shows the finite element model of elliptic cylinder gear meshing and the parameters of the elliptic cylinder gear are shown in Table 1.

Figure 4. The meshing finite element model of elliptic cylinder gear

TABLE 1. Elliptic cylinder gear design parameters

Parameter	Value
Module m(mm)	3
Number of teeth z	47
Center distance a(mm)	145
Addendum coefficient *ha**	1
Top clearance coefficient *C**	0.25
Tooth width B(mm)	30
Eccentricity *e*	0.3287
Pressure angle(°)	20
Equation of pitch curves	$r=\frac{64.667}{1\pm 0.3287\cos\varphi}$

3. ANALYSIS OF STATIC CONTACT MESHING CHARACTERISTICS OF ELLIPTIC CYLINDER GEARS

For the elliptic cylinder gears having different tooth profiles, it is difficult to analyze the distribution of stress, strain and pressure during the tooth meshing process. Static analysis should be carried out first to find the key parts of the stress, strain and pressure distribution during the meshing process. The distribution of the contact state, tooth surface friction, slip distance, contact vibration, tooth meshing contact gap and tooth contact penetration of a single tooth under the condition of 2D contact is obtained by ANSYS software, as shown in Figure 5.

In Figure 5a, the pitch curve and the vicinity of the root are in the sticking state of driving wheel (left gear), which means that the amount of wear here is the largest during the tooth engagement. The tooth surface friction distribution state in Figure 5b shows the largest near the pitch curve, and the transition from the pitch curve to the root and the tip of the tooth is reduced. Figure 5c shows the slip distance during the tooth meshing, and the slip between the driving and driven wheels is also the largest near the pitch curve. Due to certain vibration generated during the tooth meshing process, the friction between the two tooth surfaces during the meshing process will transfer the vibration to the non-contact area, the other part except the pitch curve, as shown in Figure 5d. The vibration amplitude of the top and root regions is larger, and the vibration amplitude near the pitch curve is smaller. Figure 5e shows the distribution of the contact gap during the tooth meshing process. In the vicinity of the pitch curve, the contact gap is almost 0, indicating the teeth are in meshing state. During the meshing process, the frictional force in the vicinity of the pitch curve are larger than that in the top and root of the tooth. That is to say, the amount of wear in the vicinity of the pitch curve is also the largest. In order to prove this, the tooth meshing contact penetration as shown in Figure 5f is obtained. Here the meshing penetration in the vicinity of the pitch curve is larger than the top and the root portion of tooth. Therefore, in the process of subsequent analysis of the tooth meshing error, the area near the pitch curve should be mainly analyzed.

The relationship between cumulative iteration number and absolute convergence norm can be used to show the convergence under certain convergence criteria. The convergence criterion of the finite element simulation used in this analysis is 2-norm, as show in Figure 6, the purple line represents the residual, and the blue line represents the convergence criterion. When the residual is dipped below the convergence criterion, it represents convergence.

4 DYNAMIC MESHING CHARACTERISTICS ANALYSIS OF ELLIPTIC CYLINDER GEARS

When simulating the meshing process, the following boundary conditions should be set: the inner ring of the rigid body shaft hole drives the gear body to rotate, the gear material is Solid-164 flexible body, the inner hole of the shaft is Shell-163 rigid body, density is $7.8\times10^{3}\,\mathrm{kg}/m^{3}$, the modulus of elasticity is 201Gpa and Poisson's ratio is 0.3. The driving and driven wheels are limited to X, Y, Z three-direction moving degree of freedom and X, Y rotation degrees of freedom, and the driving speed of the driving wheel is 600r/min. In the process of solving the tooth meshing model, the time step and the scale factor of the calculation time step are too large to interrupt the simulation, while the generation of negative volume is mostly caused by grid distortion, which is related to mesh quality and material and load conditions. Therefore, the appropriate time

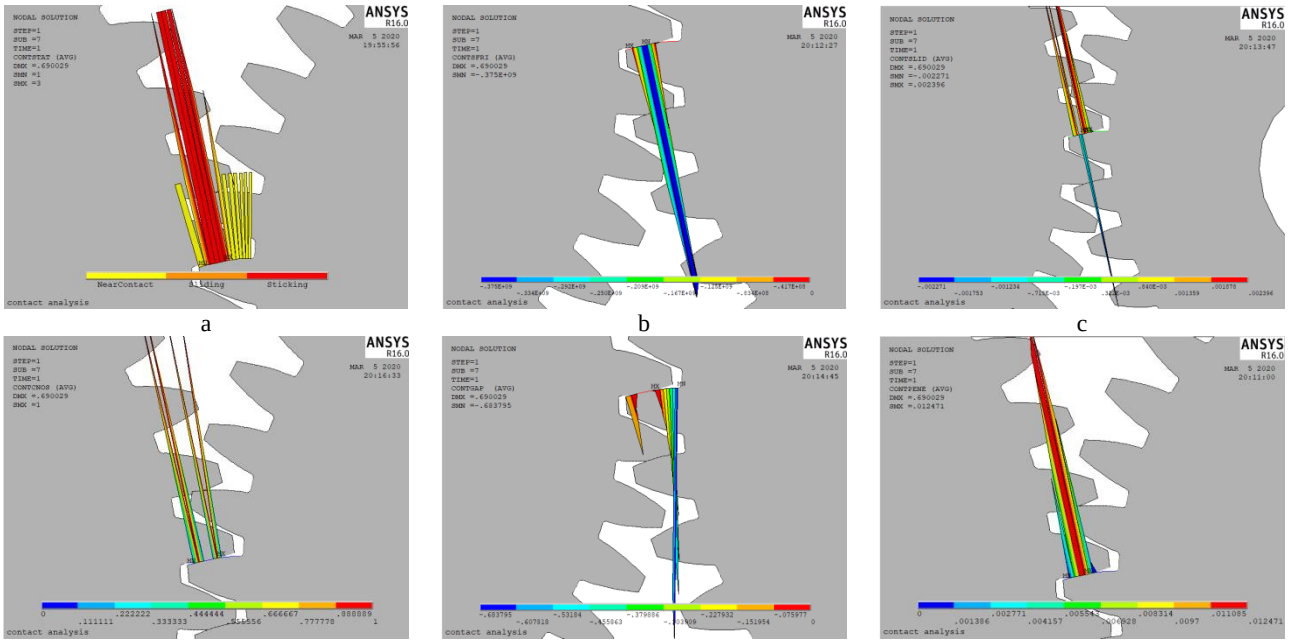

Figure 5. Static analysis of elliptic cylinder gear meshing a tooth contact state, b tooth surface friction, c meshing slip distance, d tooth contact vibration, e tooth contact gap, f tooth contact penetration

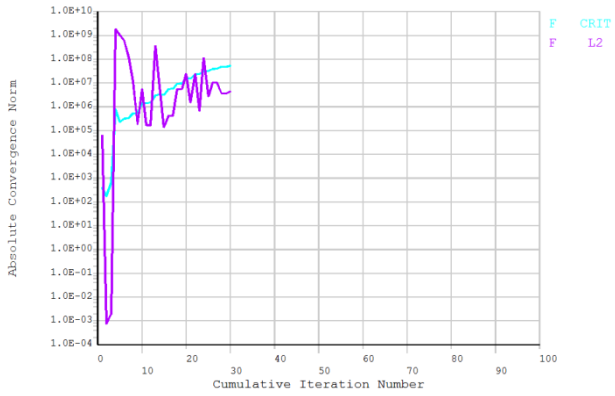

Figure 6. Convergence of finite element analysis

step should be taken to avoid the negative volume. The debug time step scale factor TSSFAC is taken the value of 0.5, the time step DT2MS values -2×10^{-7} can complete the analog tooth engagement. After meshing, the number of driving wheel nodes is 205,716, the number of units is 210,211, the number of driven wheel nodes is 181,740, and the number of units is 186,180. [18]

The tooth surface contact area during the meshing of the elliptic cylinder gears exhibits an elliptical shape, which is similar to the tooth surface contact area of the spur gear, indicating that the stress and strain of the this region is greatest during the tooth meshing process. Therefore, in the subsequent analysis of the meshing error of the elliptic cylinder gear, the meshing elements of the driving and driven wheel pitch curves and the middle section are selected as the research objects. Since the tooth profiles of the elliptic cylinders are different, it is difficult to analyze the data of all the teeth. For this reason, six teeth are selected as the research object in the analysis process, selecting No.1 tooth near the shaft hole and No.5, No.10, No.15, No.20 and No.24 teeth in the clockwise direction, as shown in Figure 7.

4. 1. Comparative Analysis of Effective Plastic Strain of Teeth Gear wear is very complicated, and it is related to various conditions such as working conditions, lubrication conditions, tooth surface roughness, etc. In the process of simulating, the degree of wear of the gear can be reflected by amount of the effective plastic strain of the tooth surface. By collecting

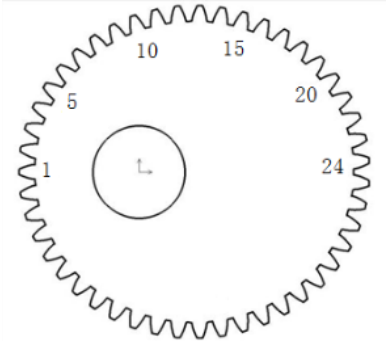

Figure 7. Tooth Number

the meshing data of the same meshing unit of driving and driven gear, the variation law of effective plastic strain during the tooth meshing process can be obtained, as shown in Figure 8. The effective plastic strain of the driving wheel is larger than that of the driven wheel, and will change due to the position of the teeth on the pitch curve. The effective plastic strain of the teeth at the ends of the short axis and its vicinity is larger than that at both ends of the long axis and its vicinity, which indicates that the amount of wear of the driving wheel is greater than that of the driven wheel during the tooth meshing process.

The presence of lubricant between the teeth during meshing reduces the wear between the teeth and accelerates the transmission of the heat generated by the meshing between the teeth, but does not eliminate the wear between the primary and driven wheels. The presence of the impact causes the driving wheel to wear more than the driven wheel. Therefore, it is conceivable to distribute the gear with higher manufacturing precision at the driving wheel during the mounting process.

4. 2. Comparative Analysis of Tooth Effective Stress Through the solution of the finite element model of the elliptic cylinder gear, the distribution area of the effective stress of the tooth surface is obtained, as shown in Figure 9, which shows that the contact area of the tooth surface in the process of

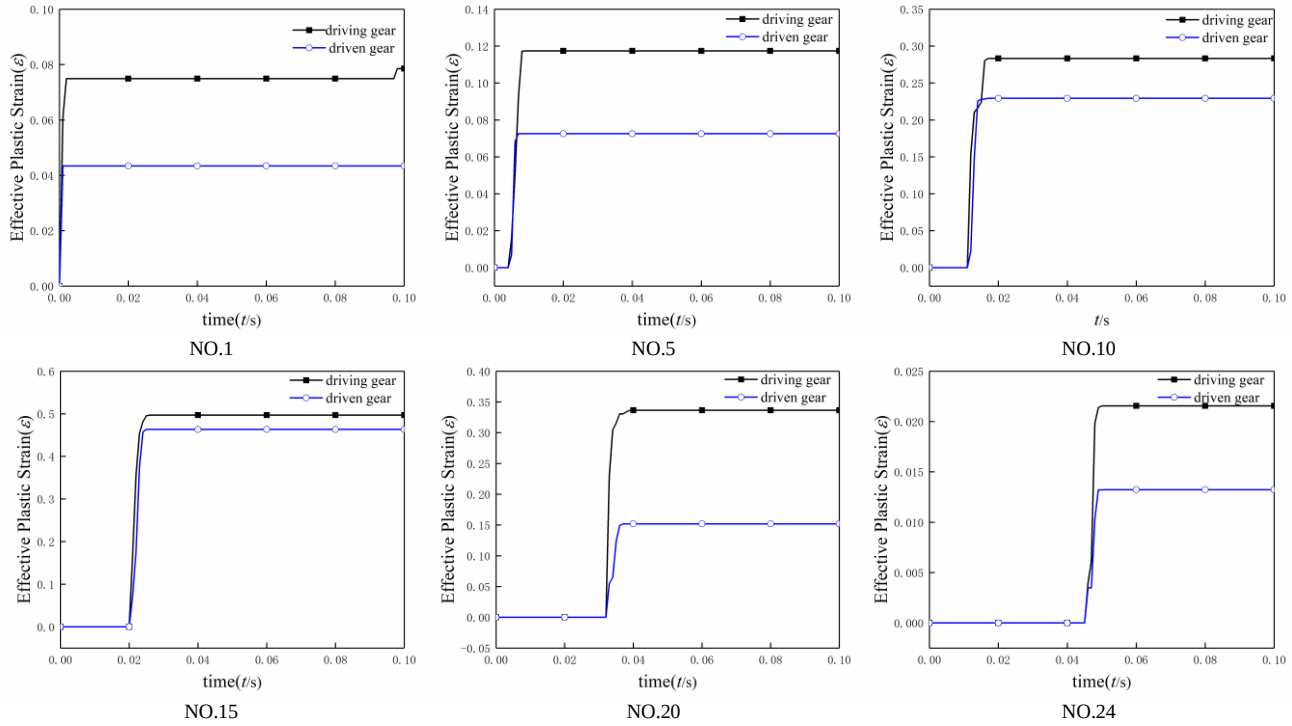

Figure 8. Effective plastic strain of the tooth data collection point

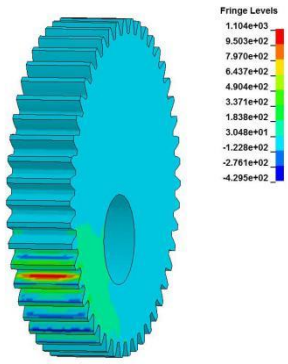

Figure 9. Effective stress distribution of tooth surface

gear engagement is also elliptical and consistent with the analysis in the literature [18-22], which further verifies the accuracy of the analysis method proposed in article.

Figure 10 shows the distribution of the effective stress of the six teeth. The effective stress curve of the driving wheel is smoother, and there is a certain impact in that of driven wheel. The occurrence of the impact is synchronized with the driving wheel, but the amplitude is larger than that of the driving wheel, which indicates that there is a certain meshing impact in the tooth meshing process. In the initial meshing phase, the effective stress curves of the driving and driven wheels have a large impact (biting impact), and the meshing

time also changes with the position of the teeth on the pitch curve. The impact will have a certain backward movement with the position of the teeth. After the withdrawal of the mesh, the stress on the teeth does not decrease to 0 due to the residual stress, but fluctuates within a certain range of values. The residual stress experienced by the driving and driven wheels will vary with the position of the teeth on the pitch curve. In the theoretical state, the interaction of forces and the interaction of deformation indicate that the effective stress between the teeth of the same pair should be the same. However, the presence of the flank clearance and power loss will cause the stresses and strains of the driving and driven teeth to be different during the meshing process, and the difference can be approximated to the calculated value of the meshing error of the teeth [11]. The residual stresses, produced in the contact region, is a key step in determination of the continuing integrity of engineering and structural components, and the literature [23-24] have been described in detail, and will not be described here.

Table 2 shows the fluctuation values of tooth effective stress. The fluctuation values of No. 1 tooth and No. 5 tooth are several times larger than that of the other teeth. The reason is that the center of the gear rotation is located at the left focus of the elliptical curve, and the driving gear mesh with the teeth near the focus are located near the right focus of the elliptical curve. The tooth at the position and the left focus has the smallest force arm and the largest meshing force, which causes the material deformation to increase and the effective stress to increase. The increase in the amount of tooth wear during the meshing process causes the meshing error to become large.

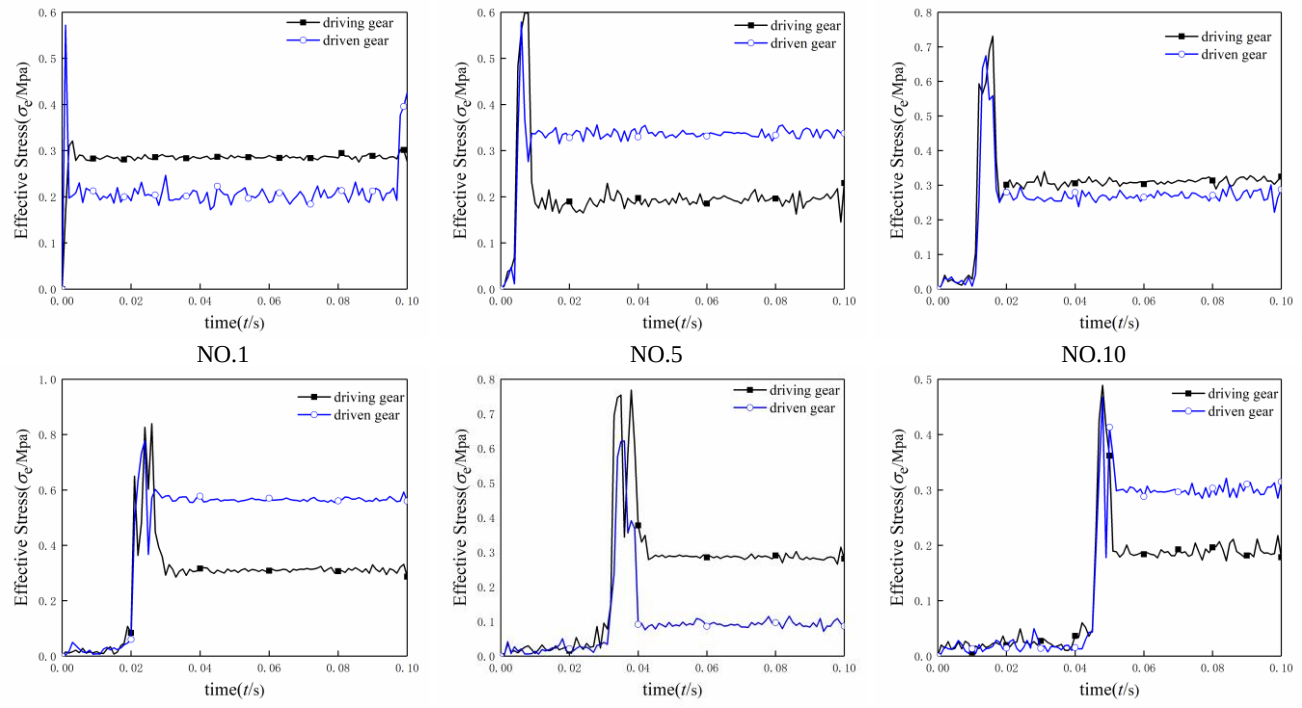

Figure 10. Effective stress of tooth data collection point

TABLE 2. Fluctuation value of tooth equivalent stress

Number	Δ Driving	Δ Driven	Fluctuation value
1	19.174	74.185	55.011
5	66.621	40.712	25.909
10	53.787	63.102	9.315
15	45.988	37.352	80636
20	36.704	44.126	7.422
24	45.84	36.684	9.156

4. 3. Comparative Analysis of Tooth Surface Contact Pressure Figure 11 shows the trend of the pressure on the same engagement unit of the driving and driven wheels. The pressure curve is always continuous, which indicates that the teeth have good contact characteristics and no tooth separation occurs. In the initial meshing stage, due to the existence of the meshing impact, there will be a certain collision between the teeth, which is specifically shown as the impact phenomenon on the left side of the pressure curve. Since the teeth are different in position on the elliptical pitch

curve, the meshing time will also be slightly different. Therefore, the phenomenon of impact on the left side of Figure 11 will have a certain right shift.

In Figure 11, only No.1 and No.24 teeth have a slight impact on the pressure curve, and the other tooth pressure curves have only a small range of fluctuations. The reason for this phenomenon is that No. 1 tooth and No. 24 tooth are respectively located at both ends of the long axis in the elliptical pitch curve. Due to the change of the radius of the pitch curve during the tooth meshing process, the teeth will generate a certain meshing vibration and impact, and the pressure curve will be reflected in the form of small fluctuations. The fluctuation of the pressure between the driving and driven wheels as shown in Table 3, was obtained by collecting the gear meshing data. In Table 3, except for No. 1 tooth and No. 20 tooth near the end points of the long axis, the fluctuation values of the other four teeth are relatively stable. In contrast, the fluctuation value of the driving wheel is larger. The fluctuation of the surface pressure is reflected in the form of vibration and impact in the specific working conditions, and the inconsistency of the pressure fluctuation between the driving and driven wheels indicates that the meshing error between the teeth also changes at the moment momentarily, and is decreased with the transition of the long axis of the elliptic pitch curves to the short axis.

4. 4. The Influence of Load on Tooth Meshing Error In order to study the influence of the load on the tooth meshing error, the change in effective plastic strain, effective stress and surface pressure of No. 1 tooth under normal load and alternating load were obtained respectively, as shown in Figure 12. Under the

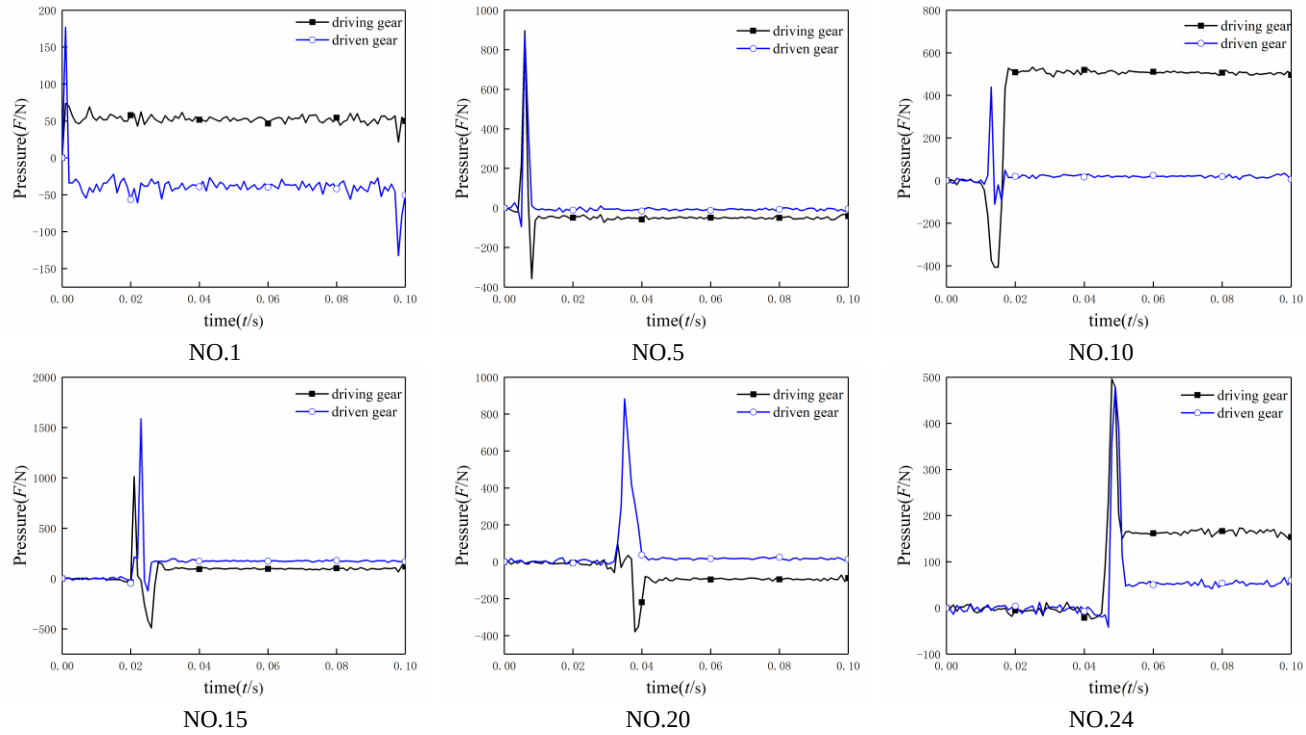

Figure 11. Tooth surface pressure of the data collection point

TABLE 3. Fluctuation value of tooth surface pressure

Number	Δ Driving	Δ Driven	Fluctuation value
1	26.187	38.774	12.557
5	39.472	31.26	8.212
10	45.767	42.882	2.885
15	43.858	37.72	6.138
20	42.365	16.422	25.943
24	19.345	24.768	5.428

condition of alternating load, the effective plastic strain of the driving and driven wheels is larger than that of the normal load, which indicates that the meshing conditions of the teeth are more complicated under the condition of alternating load. In terms of effective stress, the alternating load, due to its time-varying, causes the material strains to cancel each other during the tooth meshing process, which makes the effective stress under the alternating load condition lower than the normal load condition. During the tooth meshing process, the effective stress and surface pressure change under

normal load conditions are relatively stable. In contrast, under the alternating load condition, there is a slight impact on the effective stress curve and the pressure impact on the tooth surface increases, which indicates that the meshing error between the teeth under the alternating load condition will increase. To verify the above conclusion, the tooth surface pressure fluctuation values under the two load conditions were obtained, as shown in Table 4. Through the comparative analysis of the value of pressure fluctuation of the tooth surface, it can be known that the meshing error of the teeth is increased due to the time variation of the load under the alternating load condition.

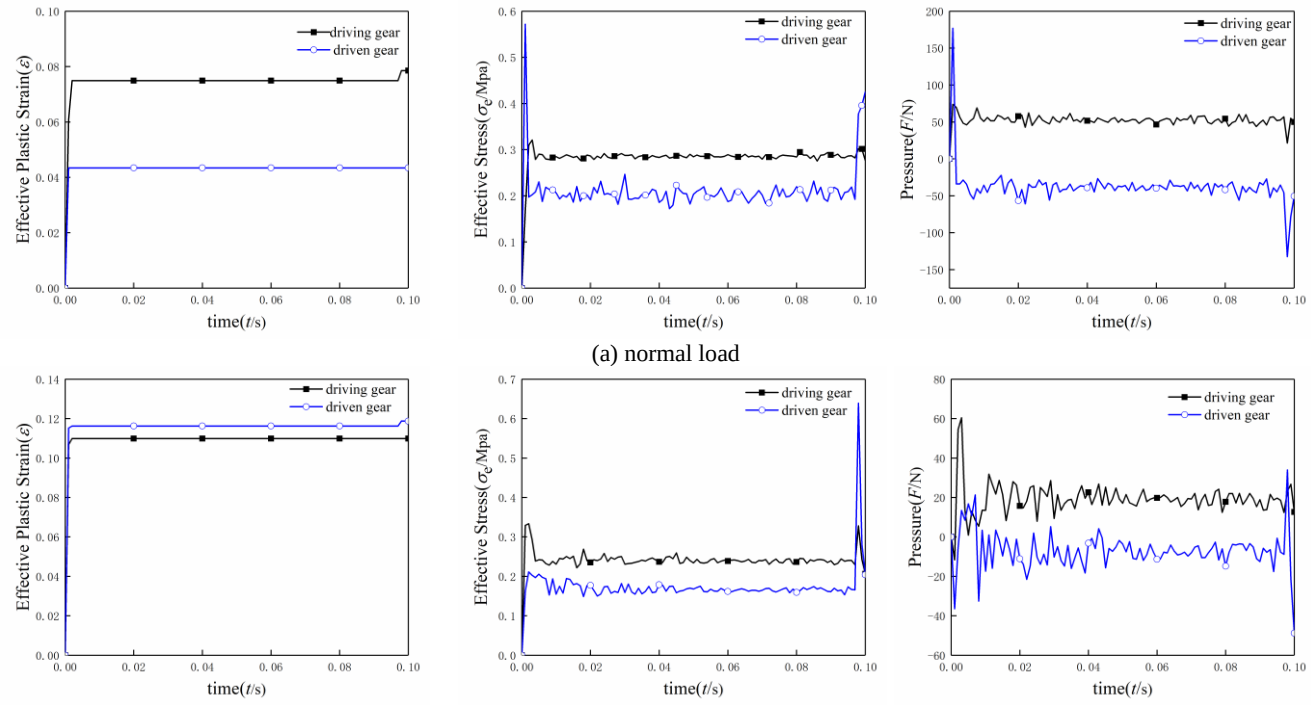

(a) normal load

(b) alternating load

Figure 12. Distribution of strain, stress and pressure of teeth under two load conditions

TABLE 4. Fluctuation values of tooth surface pressure under different load conditions

	Common load	**Alternating load**
Δ Driving	23.576	26.187
Δ Driven	37.647	38.744
Fluctuation values	14.071	12.557

5 CONCLUSIONS

For the elliptic cylindrical gear pair, the static analysis of the tooth surfaces that mesh with each other was first performed to determine the key parts of the gear meshing process. Based on this, the difference between the stress, strain, and pressure of the tooth surfaces of the driving and driven gears during the gear meshing process is proposed as a reference for describing the gear meshing error, and a dynamic meshing model of the elliptic cylinder gear is established. The distribution laws of effective plastic strain, effective stress, surface pressure and meshing error during gear meshing are obtained. The conclusions are as follows:

a) The static contact analysis of the elliptic cylinder gear pair shows that the region near the pitch curve is the key part in the process of gear meshing.

b) The effective plastic strain, effective stress, pressure on the tooth surface and the meshing error will vary with the position of the tooth on the pitch curve. Therefore, in the process of gear installation, the tooth modification can be considered or the gear with higher manufacturing precision can be distributed at the driving wheel to avoid this phenomenon.

c) Load has a certain influence on meshing error. In contrast, the alternating load causes meshing condition to be more complicated due to its time-varying characteristics, and will increase the meshing error of the gear.

d) The dynamic meshing model and meshing error analysis method proposed in this paper can be applied to other types of noncircular gears

6. ACKNOWLEDGEMENTS

This research received specific grant from the National Natural Science Foundation of China (No. 51765032)

7. REFERENCES

1. Litvin, F. L., "Noncircular gears design and generation", ***Cambridge University Press***, 2009.
2. Li R. F., Wang J. J., "Dynamics of gear system", ***Beijing: Science Press***, 1997.
3. Sainte M. N., Velex P., Roulois G., Caillet J., "A study on the correlation between dynamic transmission error and dynamic tooth loads in spur and helical gears", ***Journal of Vibration and Acoustic***, Vol. 139, (2017) ,1-10. http://dx.doi.org/10.1115/1.4034631
4. Sungho P., Seokgoo K., Joo-Ho C., **"**Gear fault diagnosis using transmission error and ensemble empirical mode decomposition", ***Mechanical Systems and Signal Processing***, No. 108, (2018), 262–275. http://dx.doi.org/10.1016/j.ymssp.2018.02.028
5. Hotait M. A., Kahraman A., **"**Experiments on the relationship between the dynamic transmission error and the dynamic stress factor of spur gear pairs", ***Mechanism and Machine Theory***, Vol. 70, No. 6 (2013), 116-128. http://dx.doi.org/10.1016/j.mechmachtheory.2013.07.006
6. Wang G. J., Chen L., Li Y., Zou S. D., "Research on the dynamic transmission error of a spur gear pair with eccentricities by finite element method", ***Mechanism and Machine Theory***, Vol. 109, (2017), 1-13. http://dx.doi.org/10.1016/j.mechmachtheory.2016.11.006
7. Yu L., Wang G. J., Zou. S. D., "The experimental research on gear eccentricity error of backlash-compensation gear device based on transmission error", ***International Journal of Precision Engineering and Manufacturing***, Vol. 19, No. 1 (2018), 5-12. http://dx.doi.org/10.1007/s12541-018-0001-7
8. Deng X. Z., Xu A. J., Zhang J., Li H. B., Xu K,. **"**Analysis and experimental research on the gear transmission error based on pulse time spectrum", ***Chinese Journal of Mechanical Engineering***, Vol. 50, No. 1 (2014), 85-90. http://dx.doi.org/10.3901/JME.2014.01.085
9. Zou S. D., Wang G. J., **"**Research on transmission error of dual-eccentric gears", ***Journal of University of Electronic Science and Technology of China***, No. 6, (2017), 157-162. http://dx.doi.org/10.3969/j.issn.1001-0548. 2017.06.027
10. Wu S. J., Peng Z. M., Wang X. S.,Zhu W. L., Li H. W., Qian B., Cheng Y., "Impact of mesh errors on dynamic load sharing characteristics of compound planetary gear sets," ***Chinese Journal of Mechanical Engineering***, Vol. 3, No. 40, (2016), 1-6. http://dx.doi.org/10.3901/JME.2015.03.029
11. Chang L. H., Liu G., Wu L. Y., **"**Determination of composite meshing errors and its influence on the vibration of gear system", ***Chinese Journal of Mechanical Engineering***, Vol.51, No.1 (2015), 123-130. http://dx.doi.org/10.3901/JME.2015.01.123
12. Sumar H. S., Athanasius P. B, Jamari., Jamari G. R., "Simulation of excavator bucket pressuring through finite element method", ***Civil Engineering Journal***, Vol. 4, No. 3, (2018), 478-487. http://dx.doi.org/10.28991/cej-0309189
13. Massoud H. E., Mahyar N., Farzad T., "Position control of a flexible joint via explicit model predictive control: an experimental implementation", ***Emerging Science Journal***, Vol. 3, No.3 (2019) 146-156. http://dx.doi.org/10.28991/esj-2019-01177
14. Abbas A. L., Mohammed A. H., Abdul-Razzaq K. S., "Finite Element Analysis and Optimization of Steel Girders with External Prestressing", ***Civil Engineering Journal***, Vol. 4, No. 3, (2018) 1490-1500. http://dx.doi.org/10.28991/cej-0309189
15. Li Q., Wu S., Q., Yan J. B, "Dynamic contact emulate analysis of logarithmic spiral bevel gear with ANSYS/LS-DYNA", ***Applied Mechanics and Materials***, Vol. 86, (2011), 531-534. http://dx.doi.org/10.4028/www.scientific.net/AMM.86.531
16. Tong H., Liu Z. H., Yin L., Jin Q., "The dynamic finite element analysis of shearer's running gear based on LS-DYNA", ***Advanced Materials Research***, Vol.402 (2012), 753-757. http://dx.doi.org/10.4028/www.scientific.net/AMR.402.753
17. Ma Y., Dong X. H., Huang Q., "Tooth root stress analysis of gear processed by full radius hob based on ANSYS/LSDYNA", ***Advanced Materials Research***, Vol.479-491 (2012), 1409-1413. http://dx.doi.org/10.4028/www.scientific.net/AMR.479-481.1409
18. Dong C. B., Liu Y. P., Wei Y. Q., "Dynamic Meshing Characteristics of Elliptic Cylinder Gear Based on Tooth Contact Analysis", International Journal of Engineering, Transactions A: Basics, Vol. 33, No. 4 (2020) 676-685. http://dx.doi.org/10.5829/IJE.2020.33.04A.19

Reze Kashyzadeh K., Farriahi G. K., Shariyat M., Ahmadian M. T., "Experimental and Finite Element Studies on Free Vibration of Automotive Steering Knuckle". International Journal of Engineering, Transactions B: Applications, Vol. 30, No. 11 (2017) 1776-1783. http://dx.doi.org/10.5829/ije.2017.30.11b.20

Francisco S. M., Jose L. I., Victor R. C., "Numerical tooth contact analysis of gear transmissions through the discretization and adaptive refinement of the contact surfaces", ***Mechanism and Machine Theory***, Vol. 101 (2016), 75-94. http://dx.doi.org/10.1016/j.mechmachtheory.2016.03.009

19. Argyris J., Fuentes A., Litvin F. L., "Computerized integrated approach for design and stress analysis of spiral bevel gears", ***Computer Methods in Applied Mechanics and Engineering***, Vol. 191, No. 11-12 (2002), 1057-1095. http://dx.doi.org/10.1016/S0045-7825(01)00316-4
20. Wang Y. M., Shao J. P., Wang X. G., Zhao X. Z., "Thermomechanical coupled contact analysis of alternating meshing gear teeth surfaces for marine power rear transmission system considering thermal expansion deformation", ***Advances in Mechanical Engineering***, Vol. 10, No. 1 (2018), 1-12. http://dx.doi.org/10.1177/1687814017753910
21. Fawwahi G. H., Faghidian S. A., Smith D. J., "An inverse approach to determination of residual stresses induced by shot peening in round bars", ***International Journal of Mechanical Sciences***, Vol. 51, No. 9-10 (2009), 726-731. http://dx.doi.org/10.1016/j.ijmecsci.2009.08.004
22. Faghidian S. A., Goudar D., Farrahi G. H., David J. S., "Measurement, analysis and reconstruction of residual stresses", ***Journal of Strain Analysis for Engineering Design***, Vol. 47, No. 4 (2012), 254-264. http://dx.doi.org/10.1177/0309324712441146

Persian Abstract

چکیده

به منظور بررسی ویژگی‌های جفت‌شوندگی پویای چرخ‌دنده‌های استوانه‌ای با مقطع بیضوی و به دست آوردن خطای انطباق در سیستم انتقال دنده، تحلیل تماس ایستای دو بعدی سطح دندانه‌ی دنده و از نرم افزار ANSYS استفاده شد و قسمت‌های کلیدی سطح تماس دندده‌ها تعیین شدند. سپس، مدل جفت‌شوندگی پویای چرخ دنده‌های استوانه‌ای بیضوی تولید شده و با استفاده از نرم افزار ANSYS LS-DYNA، فرآیند تماس پویا زیر بار شبیه‌سازی شد. قانون توزیع فشار مومسان مؤثر، تنش و فشار مؤثر چرخ‌های راننده و محرک به دست آمد. بر این اساس، قانون توزیع خطای جفت‌شوندگی از طریق محاسبه به دست می‌آید. نتایج نشان می‌دهد که توزیع تنش، کرنش و فشار سطح دندانه در حین درگیری دندانه با موقعیت آن در منحنی بیضوی گام مرتبط است. موقعیت دندانه روی منحنی گام و باری که تحمل می‌کند، تأثیر خاصی بر خطای جفت‌شوندگی دارد. نتایج این تحقیق می‌تواند راهنمایی‌هایی برای مطالعه‌ی بعدی در مورد خطای انتقال دنده‌های غیردایره‌ای، اصلاح دنده‌ها و کاربردهای مهندسی آنها ارائه دهد.